IJCS INTERNATIONAL JOURNAL OF CONSERVATION SCIENCE

ISSN: 2067-533X Volume 10, Issue 2, April-June 2019: 279-290 www.ijcs.uaic.ro

ANALYTICAL AND EXPERIMENTAL STUDY OF BLEMISHES FORMATION AND PREVENTIVE CONSERVATION OF CELLULOSE ACETATE MICROFILMS

Heba BARAKAT[1*], Enrico CILIBERTO[2], Sawsan DARWISH[3], Osama SAQR[4]

[1] Egyptian National Library and Archives, Ministry of Culture, Egypt.
[2] Chemistry Department, Catania University, Italy.
[3] Conservation Department, Faculty of Archaeology, Cairo University, Egypt.
[4] Photography, Cinematography and Television Department, Faculty of Applied Arts, Helwan University, Egypt.

Abstract

The current study is interested in evaluating the oxidation process that causing redox blemishes on processed microfilms. Images on black and white films are typically formed by metallic silver in a gelatin binder. When exposed to a combination of moisture in the environment and pollutants in the air or contaminants in the film's enclosure, this image silver will corrode. The investigation and analysis made during this work proved that the oxidation agent produced by performing the hydrogen peroxide test, influenced only the silver particles although the gelatin layer and the film base did not suffer from any oxidation. The results of FTIR-ATR showed that the base and the gelatin were affected by hydrolysis regards to the high relative humidity required for the test. Applying a sacrifice layer by sputtering coating showed good results in reducing the formation of the redox blemishes especially in the case of using copper as a sputtering target comparing to zinc for cellulose acetate film samples.

Keywords: *Cellulose Acetate Microfilm; Redox Blemishes; Hydrolysis; Oxidation; Silver Gelatin; Sputtering; Zinc; Copper*

Introduction

Photographic film consider as an important documentary material. The numerous quantity and value of microfilm records used in various fields such as financial institutions, libraries, government offices, and industrial firms have focused attention on the care of such records to make certain that they last as long as possible [1].

Recently, it was especially the occurrence of red spots on microfilms around 1960, the so-called micro blemishes, woke the awareness of pollution and its effect [2]. Peroxides are the main reason for producing redox blemishes. If the source of the peroxides is removed, deterioration will not continue. Poor cardboard and storing materials made from lignin-containing wood pulp have been identified as the culprits. Such materials produce gaseous peroxides during natural aging.

The research done by *K. Hendriks* [3] concluded that the peroxides are capable of reacting with image silver to form circular orange-colored spots of colloidal silver, a modification different from black image silver. The spread of redox blemishes on film raise the awareness regarding to its risk that cause loss of valuable information. Some chemical treatments are being tested which may also retard their spread. Minor forms of deterioration on

* Corresponding author: reshebasherif@gmail.com

film rated as fair may be corrected with approved cleaning materials such as trichloroethylene, although duplication is recommended. Refer to manufacturers' warnings when using cleaning materials.

R. Hofmann and H. Wiesner [4] identified that information loss can not be restored on film rated as bad. An inspection should be made immediately of all film with similar characteristics as the film rated as fair, poor, or bad. Poor and bad film should be duplicated immediately in order to salvage the remaining information. Because of the redox blemishes attack on microfilm images can be very damaging and can occur in relatively short time periods, the more frequent form of oxidative attack is overall fading, silver mirroring, and discoloration. *J. Reilly et al* [5] found that it is important that these hazards to photographic image preservation also be addressed. Therefore, Current study aims to characterization of redox blemishes as a phenomenon related to oxidizing and reducing agents and develop a preventive treatment to prevent oxidation of silver particles.

According to *B. Chudnovsky* [6], *P. Francis* [7] Corrosion mitigation can be achieved by utilizing a combination of a good-quality coating and a cathodic protection system. Cathodic protection can be used for preventing corrosion by converting all of the anodic (active) sites on the metal surface to cathodic (passive) sites by supplying electrical current (or free electrons) from an alternate source. Conversely, if we supply additional electrons from an external source to the piece of metal, oxidation reaction will decrease to give reduced corrosion according to the areas.

In terms of standard electrode potentials it has been possible to draw an electrochemical series indicating the oxidizing /reducing power of the oxidized /reduced state of a redox system. The standard reduction potential of an electrode is considered as the standard electrode potential. Since SHE is arbitrarily assigned the potential, $Eo(2H^+/H_2) = 0$, the electrodes in which the reduced state is a stronger reducing agent than hydrogen such as the electrode Zn^{2+}/Zn, the standard potential (reduction potential) is negative by convention. The electrodes in which the reduced state is a weaker reducing agent than hydrogen such as Cu^{2+}/Cu, the standard potential (reduction potential) is positive by convention [8]. *Z. Laughlin et al* [9] reported that Zinc and copper having the most negative standard electrode potentials therefore they are recommended for this work.

Since there was a need to replace the electrolyte to avoid any aqueous treatments since they are not recommended in case of the photographic material, applying the sacrificial anodic of zinc and copper was performed using sputtering technique. *M. Friz* [10] identified sputtering as a concept that means a physical vapor deposition (PVD) process used for depositing materials onto a substrate, by ejecting atoms from such materials and condensing the ejected atoms onto a substrate in a high vacuum environment and condensed as a film [11] on the surfaces of appropriately placed parts or substrates (Fig. 1).

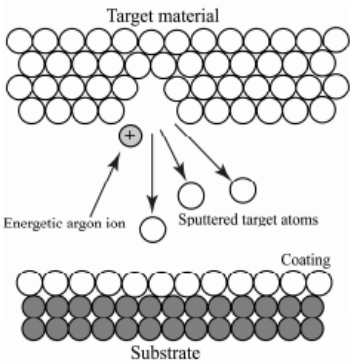

Fig. 1. Schematic of the sputter deposition process [12]

Almost all modern sputtering processes are based on magnetically enhanced cathode processes. The target is located to face the substrate, where the film grows. Positive argon ions in the plasma are accelerated towards the target, which upon impact cause a sequence of collisions in the target close to its surface [12].

Experimental

Materials

This study accomplished on samples with two different types of cellulose acetate films: 35mm microfilm roll and motion picture negative roll. Microfilm samples supplied from Akhbar-Elyoum Newspaper Archive, Egypt. The samples divided into three parts; control samples for chemical and physical investigation, samples for producing the redox blemishes and coded as oxidized samples and samples for treatment and coded as coated samples.

Sputtering Targets

Zinc and copper metal used as circular targets for sputter coating process. Sheet metals are cut with the same dimension of the target holder according to Quorum Q150R ES sputter coater which radius is 2.8cm (Fig. 2). Both targets were cleaned separately using neutral soap and distilled water. Then three ultrasonic baths were performed by using G-Sonic ultrasonic bath and 2-Propanol alcohol, each bath was for 2 minutes and finally the samples were allowed to dry. Sputtering was performed at the Chemistry Laboratory, Department of Chemical Science, Catania University, under the supervision of Prof. Ezio Viscuzo, Professor of Physics and Prof. Enrico Ciliberto, Professor of Chemistry at the University of Catania.

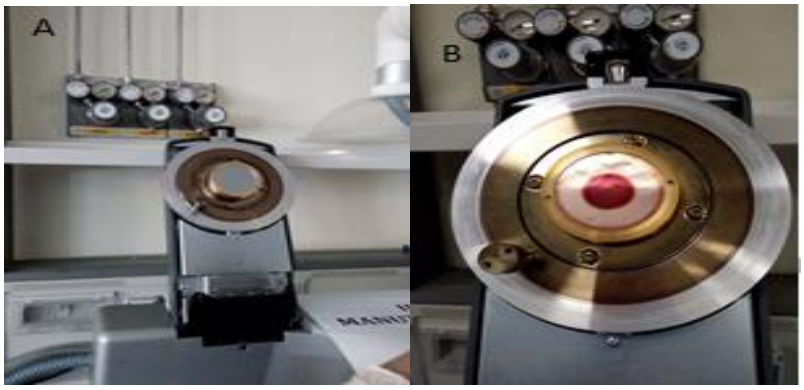

Fig. 2. Race –track formation on (A) Zinc target (B) Copper target.

Methods

Hydrogen Peroxide Test to evaluate redox blemishes formation

This test was performed twice, for formation redox blemishes for the film samples first, then for evaluated the sputtering coating applied to the film samples in an aging oven at the Chemistry laboratory in Catania University.

This procedure is relatively easy to perform and is sufficiently reliable and reproducible to study different protective treatments. One of the experiments to test this approach featured incubation of Kodak AHU microfilm for 18h. at 50°C and 82%R.H. with 2000ppm of hydrogen peroxide reported by *P. Adelstein et al* [13]. The original work on oxidative testing exposed the film to hydrogen peroxide vapor. The later modification used by Pope prepared filter paper saturated with 5% hydrogen peroxide solution which was subsequently put in the desiccator jar (Fig. 3). A modification had applied to the previous test in this study. Since the relative

humidity is one of the main factors for formation of the redox blemishes, so RH performed was 100% by using Silica Gel that completely saturated with distilled water (Fig. 4).

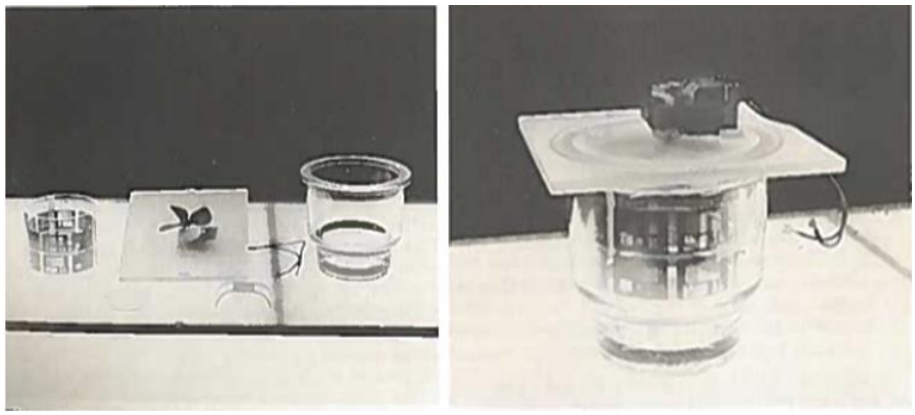

Fig. 3. Components of hydrogen peroxide test apparatus apparatus [13]

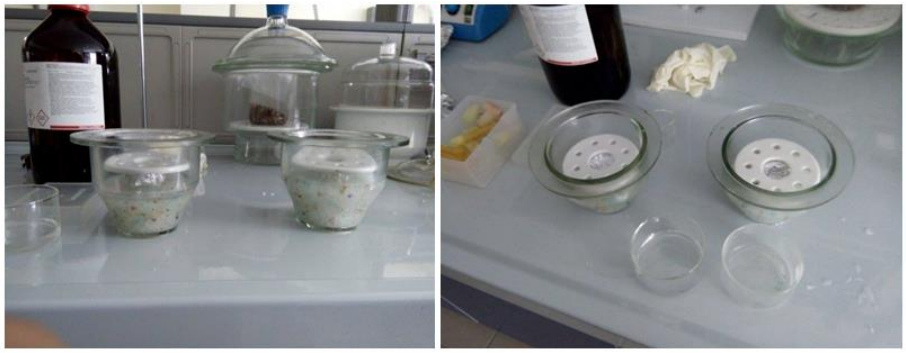

Fig. 4. Two desiccator jars are used for hydrogen peroxide test. Inside each jar small piker was located to contain the filter paper soaked in 5% hydrogen peroxide solution.

Magnetron Sputtering

Quorum Q150R ES sputter coater was used for this experiment. Sputtering process was performed under an Argon gas flow at a working distance of 50mm at 2×10^{-7}mbar for 30, 60 and 90 seconds as mentioned before.

FTIR Spectroscopy: Attenuated Total Reflectance (ATR-FTIR)

The spectra were recorded with an IR spectrometer model "Spectrum two" (Perkin Elmer) with the Universal ATR Sampling Accessory in reflectance mode, 16 scans were collected for each spectrum in the range of 4000 - 450cm^{-1}. A background spectrum was also collected under the same conditions. The analysis was performed at the chemistry Laboratory, Department of Chemical Science, Catania University.

SEM-EDX Analysis

Samples were imaged using a VP LEO 1550 SEM instrument with a field emission source and controlled electron energy of 15keV. Samples were coated by gold using Quorum Q150R ES sputter coater. Sputtering process was performed under an Argon gas flow at a working distance of 50mm at 2×10^{-7}mbar of 40mA for 30sec. SEM was performed at the SEM Laboratory, Department of Chemical Science, Catania University. Moreover, another SEM analysis performed for the oxidized samples using J OEL JSM S400LV EDX Lin l ISIS-Oxford

high vacuum at SEM lab, Faculty of Science, Assiut University. Elemental analysis performed using 10mm^2 SDD Detector to analyse the oxidized samples deteriorated by redox blemishes also for the samples treated with sputtering coating. The analysis was performed at the SEM Laboratory, Department of Chemical Science, Catania University.

Sputtering process was performed first to evaluate the efficiency of the targeted treatment; an experiment was designed to compare the sputtering time effect of both different metal of coating sputtering. White paper used to monitor any visual changes especially any change of color before applying the sputtering on the film samples. To determine the effect of treatment duration, each of the two variants was tested at three different time intervals "30 seconds, 60 seconds, and 90 seconds".

X-ray Photoelectron Spectroscopy (XPS)

XPS measurements were carried out using a PE-PHI ESCA/SAM 5600 monochromator system s with an analysis chamber base pressure of 5×10^{-10} Torr. X-ray photoemission measurements were performed using a MgKα (hν =1253.6eV) source. Analyses were carried out with a photoelectron angle of 45° (relative to the sample surface) with an acceptance angle of 7°. The energy scale of the spectrometer was calibrated with reference to the Ag3d3/2 = 368.3eV photoelectron line. Binding energies were calculated with respect to the C1s ionization at 285.00eV from adventitious carbon that is generally accepted to be independent of the chemical state of the sample under investigation. The analysis was performed at the XPS Laboratory, Department of Chemical Science, Catania University.

Results and Discussion

Visual Inspection

The results of the hydrogen peroxide test revealed the deterioration occurred to the film samples. The redox blemishes were formed as reddings in the background and distorted to fill the space between characters or lines on cellulose acetate film samples (Fig. 5). As for the sputtering coating experiment, both copper and zinc film coated samples showed good stability to oxidation agents and only slight yellowing was observed in both cases. The film sample that coated by copper was in good condition with very slight yellowing.

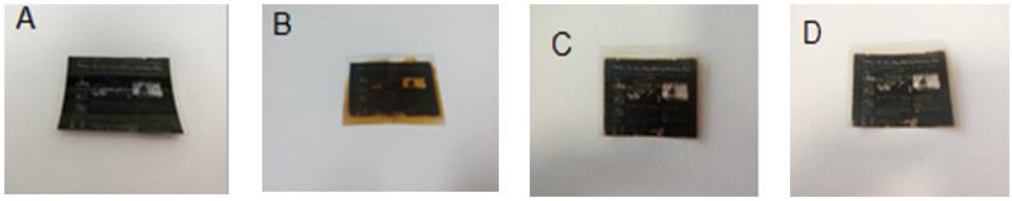

Fig. 5. The comparison status of CA samples. (A) Presents the CA control sample. (B) Shows the formation of redox blemishes after performing H2O2 Test. The sputtering coating by Zn shows in coated sample (C) and by Cu in coated sample (D).

Digital Microscope

The results of the investigation by using digital microscope showed the physical decay for the controlled samples. In addition, the examination of oxidized samples (Fig. 6) showed the oxidation mechanism resulting in the formation of redox blemishes after performing the hydrogen peroxide test. Moreover, the comparison of results between sputtering coating by copper and zinc showed that the efficacy of the copper in preventing oxidation and reducing the formation of redox blemishes on film samples.

FTIR Spectroscopy: Attenuated Total Reflectance (ATR-FTIR)

(ATR-FTIR) for Cellulose Acetate Film

Cellulose Acetate Film (Bright Side) - The film type is confirmed by IR spectroscopy. The characterization spectrum is of the control sample before performing the hydrogen peroxide test shows the typical frequencies corresponding to cellulose acetate as following: 1738cm^{-1} (C=O st), 1367cm^{-1} (CH_3 sym def), 1215cm^{-1} (C-O st), 1031cm^{-1} (C-O-C st) [14]. The compared spectra (Fig. 7) between the control samples and the samples affected by hydrogen peroxide test revealed that the film base was affected by hydrolysis (Table 1).

Fig. 6. The oxidized samples: a - Physical decay of the CA controlled samples shows appearing of 'Cinch' marks caused by the action of film moving against itself in the roll; b - CA oxidized sample show the formation of redox blemishes type 4; c - CA sample coated by zinc. It shows the oxidizing of silver particles and forming redox blemishes; d - CA sample coated by copper. It shows a good stability and reducing of oxidizing of silver particles.

Table 1. Comparison between cellulose acetate bright side- shadow and highlight areas before and after **H_2O_2** Test.

Sample	**Bright White Wavenumber cm^{-1}**		**Bright Black Wavenumber cm^{-1}**	
	Before H_2O_2 Test	**After H_2O_2 Test**	**Before H_2O_2 Test**	**After H_2O_2Test**
	3509.31	**3454.95**	**3509.31**	**3454.95**
Broad absorption bands are due to intermolecular hydrogen bonded O-H stretching. It is noticed that the intensities of these bands increased and the frequencies were shifted to lower wavenumber after ageing in both black and white samples. These decreases were due to water absorption during H_2O_2 Test and formation of more hydrogen bonds.				
	2959.33	**2939.16**	**2959.33**	**2939.16**
These bands were attributed to CH stretching of CH_2 groups (Pielesz & Binias, 2010). It was found that the frequencies decreased after performing H_2O_2 Test.				
	1738.82	**1737.99**	**1738.82**	**1737.99**
C=O stretching of ester group of acetate. The intensity of these bands decreased after performing H_2O_2 Test. Some ester bonds were hydrolyzed because of H_2O_2 Test effect especially in bright side-highlight area sample.				
		1634.57		**1635**
New bands appeared after performing H_2O_2 Test at ≈ 1635 cm^{-1}. These bands are attributed to water deformation.				
	1488.59	**1488.29**	**1489**	**1488.18**
	1433.84	**1432.93**	**1433.79**	**1433**
	1367	**1367.54**	**1367**	**1368**
CH_2 scissoring and OH bending vibrations: (Biswal & Singh 2004). The intensities of these bands increased after performing H_2O_2 Test.				
	1215.79	**1215.69**	**1215.94**	**1214.88**
C-O stretching of C-O ester and C-O-H groups. The intensity of these bands slightly decreased after performing H_2O_2 Test, especially in bright side-highlight sample as some ester groups were hydrolyzed and some C-O bonds were broken down.				
	1034.84	**1033.82**	**1035.10**	**1033.97**
C–O–C stretching of ether linkage from the glycosidic units. This band increased in bright side-shadow area sample after performing H_2O_2 Test due to crosslinking reaction.				

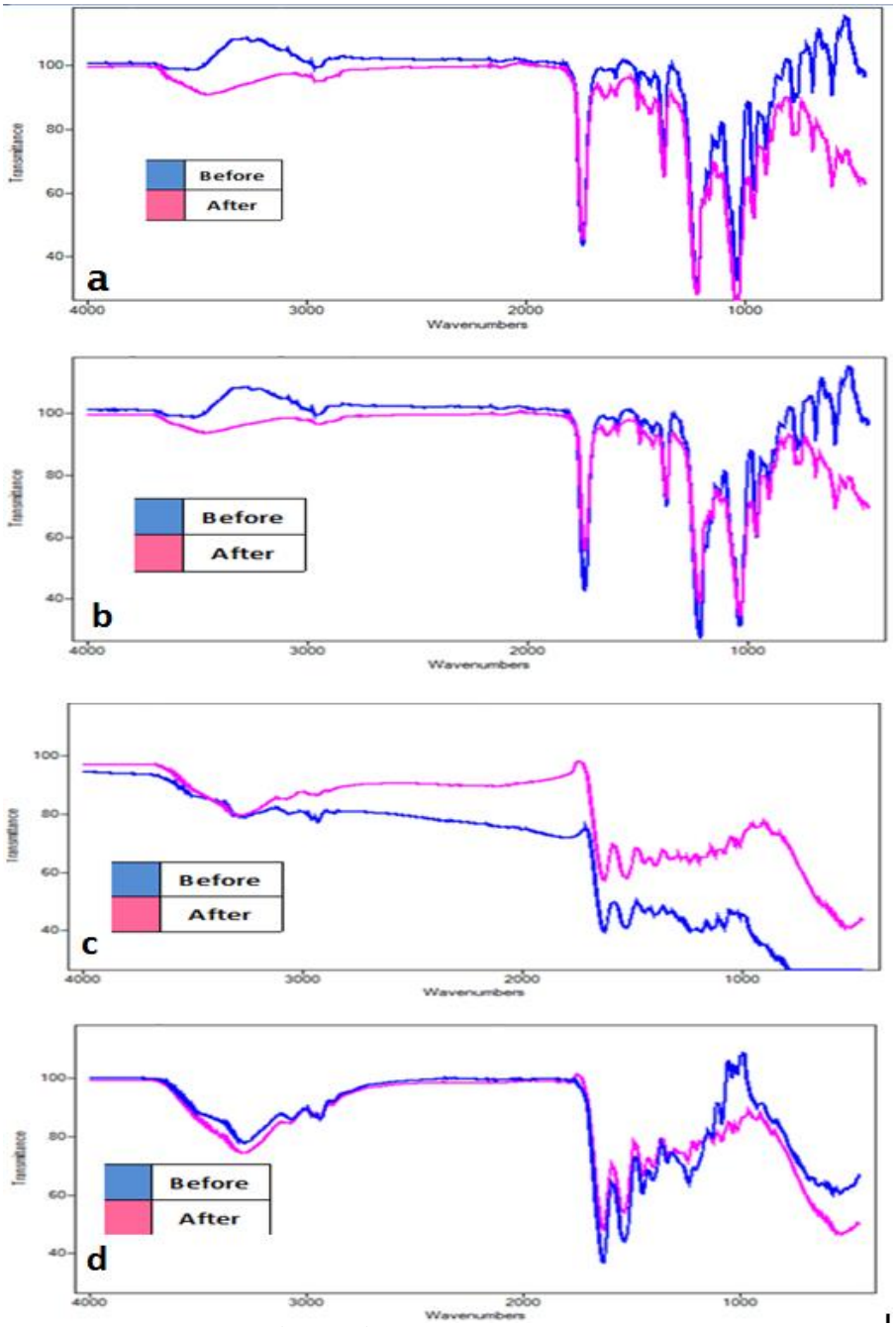

Fig. 7. FTIR-ATR spectra before and after H_2O_2 test: a - cellulose acetate bright side Shadow area; b - cellulose acetate bright side highlight area; c - cellulose acetate matt side-shadow area; d - cellulose acetate matt side-highlight area

Cellulose Acetate Film (Mat Side) - According to *M. Derrick* [15] the Protein spectra are characterized by amide stretching and bending vibrations. The amide I and II bands are the two most prominent vibrational bands of the protein backbone [16]. The compared spectra between the control samples and the samples affected by hydrogen peroxide test revealed that the gelatin layer was affected by hydrolysis (Table 2).

Table 2. Comparison between cellulose acetate mat side-shadow and highlight areas before and after H_2O_2 test

Sample	Matt white Wavenumber cm^{-1}		Matt black Wavenumber cm^{-1}	
	Before H_2O_2 Test	**After H_2O_2 Test**	**Before H_2O_2 Test**	**After H_2O_2Test**
	3285.61	**3285.98**	**3509.31**	**3280.52**
O-H stretching + N-H stretching. Bands of aged samples showed a slight wideness and increase in their intensities resulting from water absorption during H_2O_2 Test process.				
	2934.41	**2936.30**	**2926.93**	**2935**
C-H stretching				
	1631.29	**1630.99**	**1627.53**	**1628.06**
C=O stretching (Amide I). Intensities of these bands decreased after performing H_2O_2 Test.				
	1537.91	**1537.33**	**1531.84**	**1530.57**
C-N stretching + N-H bending (Amide II). Intensities of these bands decreased after performing H_2O_2 Test.				
Amide I / Amide II ratio*	0.83	0.88	0.97	0.98
	1450.80	**1451.69**	**1446.60**	**1446.56**
C-H bending.				
	1237.10	**1241.32**	**----**	**1238.0**
	1202.0	**1200.50**	**----**	**1198.0**
C-N stretching + N-H bending (amide III)				
	1128.60	**1125.0**	**1131.65**	**1124**
	1082.77	**1082.16**	**1082.32**	**1081.00**
	1035.32	**1033.41**	**1041**	**1031.58**
C-O stretching				

* Hydrolysis of the polypeptide chain would be apparent as an increase in the OH stretching or bending frequencies found at ≈ 3,280 and &1,630 cm^{-1}, respectively. Since the amide I band also occurs in the region 1,615–1,650cm^{-1}, an increase in the OH band at 1650 cm^{-1} would result in an increase in the absorption intensity or height of the amide I band. By comparing the relative absorption intensities of the amide I band to that of the amide II, we found that in the spectrum of aged samples, the amide I band is higher than the amide II.

Scanning Electron Microscope (SEM)

The results obtained from SEM investigation showed that the redox blemishes of the silver gelatin films were always accompanied by a migration mechanism resulting in the formation of small silver particles. When compared to oxidizing agents and relative humidity, have the most aggressive effect on the size and distribution of the silver particles and for the gelatin layer for cellulose acetate film samples (Fig. 8).

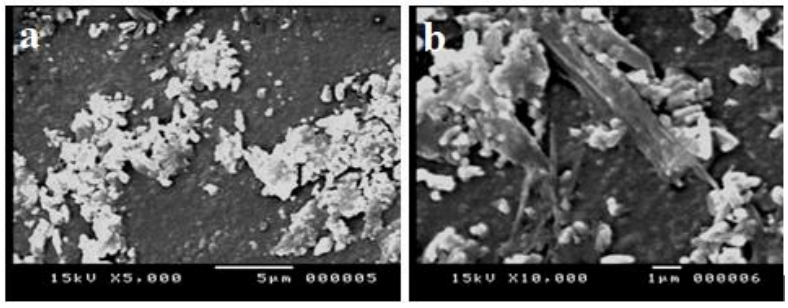

Fig. 8. SEM images: a- silver grains from CA oxidized sample at magnification 5000 X (The image shows the erosion of silver particles and the breakdown of silver particles and the formation of numerous silver particles in new sites); b- gelatin binder of CA oxidized sample at magnification 10000X (The gelatin is deteriorated because of the hydrolysis process and the effect of oxidation agents)

Energy-dispersive X-ray spectroscopy (EDX)

The results of elemental analysis of controlled samples detected the presence of carbon, oxygen, calcium, sodium, potassium, and sulfur that forms the gelatin binder layer and its impurities besides silver particles (Fig. 9). *M. Valverde* [17] found that acetate film is obtained from the cellulose fibers of cotton linters. During the process of acetylation (treating cellulose with acetic anhydride and a catalyst), acetyl groups are grafted onto the cellulose molecules. The sulfuric acid combined quantitatively with the cellulose in the intermediate stages of acetylation [18]. The acid generally builds up slowly in the film base. When enough acetic acid has been produced, the chemical process becomes autocatalytic, and proceeds much more quickly [19] and this can explain the presence of sulfur in the film sample analysis. EDX analysis was performed for samples of paper that coated with copper and zinc to assay the most convenient sputtering coating time for each target. The results showed that in the case of 30 seconds for both targets, there was not a satisfied amount either for copper or for zinc. Also in case of 90 sec., there was a slight change of color detected to grayish. As per of the previous results, it is decided to performing sputtering coating for controlled samples for only 60 sec. to avoid any change of color and to applying a convenient layer that can prevent the oxidation of the silver particles.

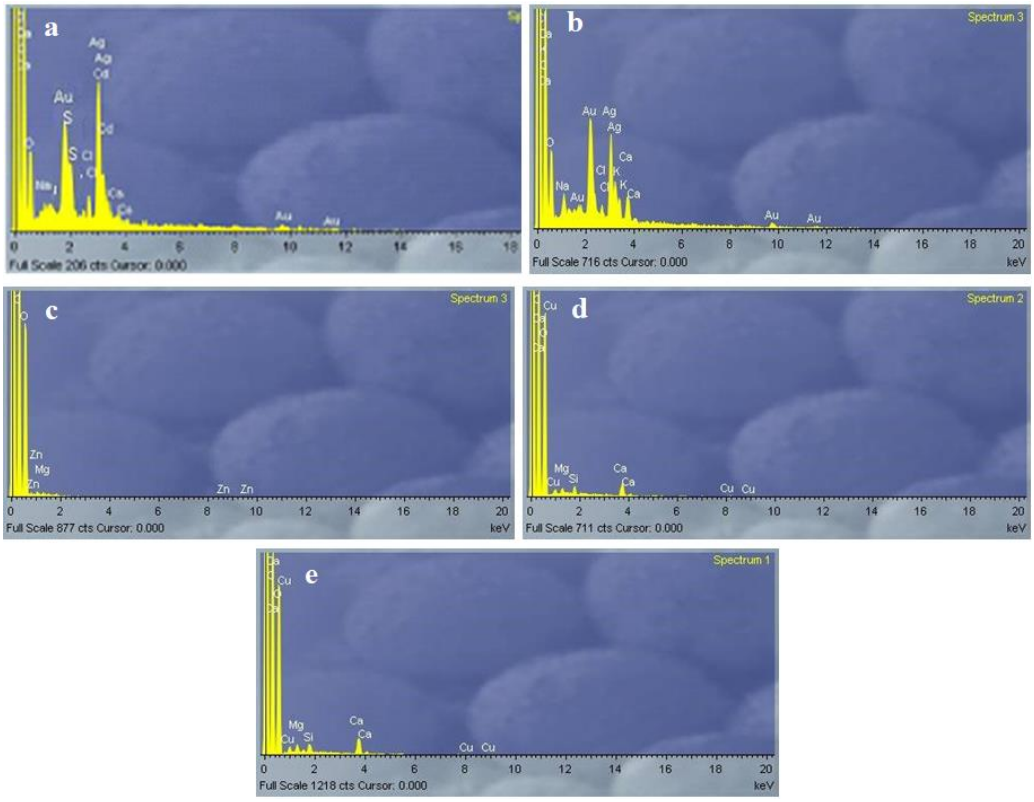

Fig. 9. EDX Spectrums: a - CA samples reveal the presence of Ag in big quantity before performing the H_2O_2 test, b - samples with redox blemishes; c - paper samples reveal the presence of zinc in a very small quantity showing results of 30 sec. sputtering coating with zinc target; d - aper samples reveal the presence of copper in a small quantity showing results of 60 sec. sputtering coating with copper target; e - paper samples reveal the presence of copper in a bigger quantity comparing to the previous spectra, showing results of 90 sec. sputtering coating with copper target

X-ray Photoelectron Spectroscopy (XPS)

Wide XPS spectrum of the controlled samples are show in (Fig. 10). This spectrum can only provide information about elemental composition of the photograph surface. In particular in the case of this sample that corresponds to a grey area that does not show any degradation process, the signals corresponding to C 1s, O 1s, Ag 3d, Ca 2p, Ca 2s, Si 2p, Si 2s, N 1s, are detected.

The very weak intensity of the silver 3d and nitrogen 1s signals indicate that the binder layer containing the silver micro-particles is coated by a protective film. The presence of silicon signals originating from the ionizations of 2p and 2s orbitals strongly indicate that the coating was obtained with a silicone polymer. In the Figure 10 are shown the XPS expanded regions from 340 to 410 eV. In this region, from lower to higher binding energies, the signals from calcium 2p, silver 3d and nitrogen 1s are evident. .

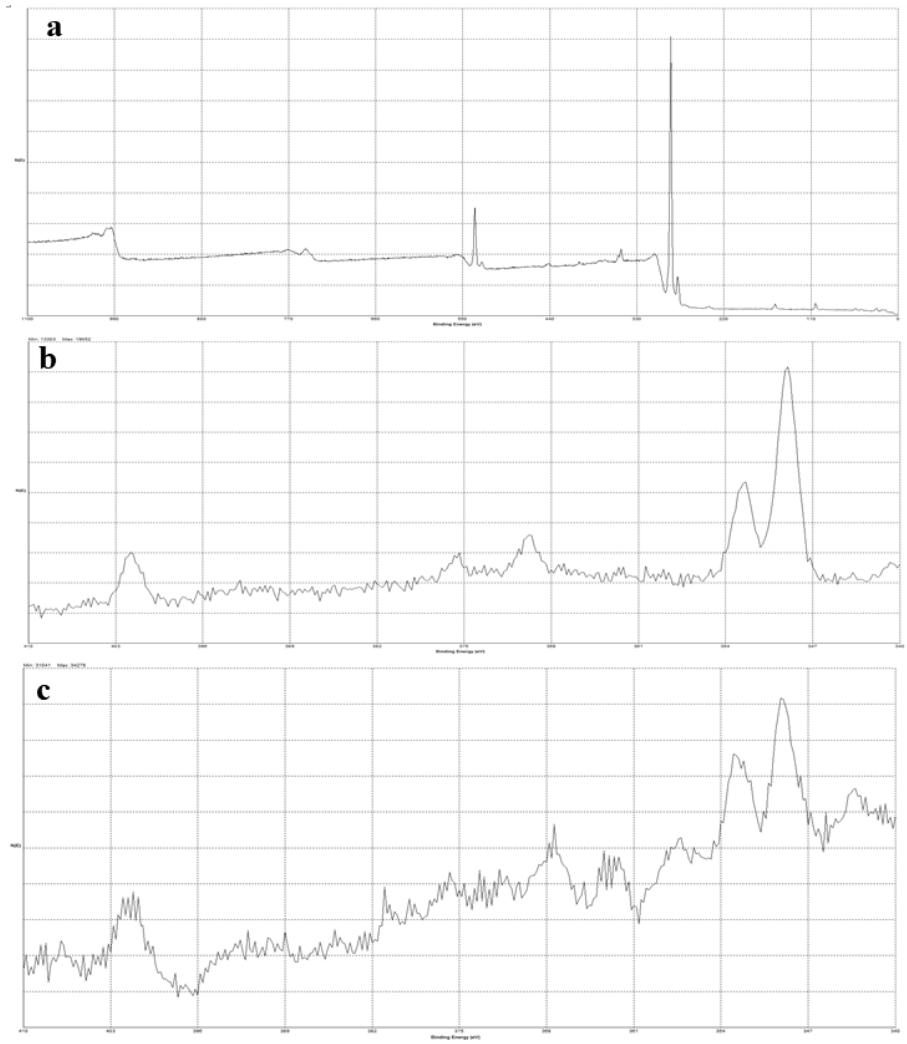

Fig. 10. XPS Spectrums: a - Wide XPS spectrum obtained from the surface of the CA controlled sample; b - XPS region from 340 to 410 eV obtained from the controlled sample; c - XPS region from 340 to 410 eV obtained from an oxidized sample in a reddish area.

It is evident that the region of the silver ionizations, that is in the range 360-380eV, is extremely more complicate in the case of the aged sample. Even if the silver signal is very low we can say that an oxidation of the silver took place. The reddish colour of the degraded areas can so be explained with a strong decrease of the size of the silver particles because of their oxidation that produce Ag+ ions able to migrate through the gelatine laye [20]. Moreover we can say that the nitrogen signal at 400eV remain also after the H_2O_2 Test process. This represents evidence that the amide groups inside the gelatine network do not suffer any oxidation under the condition of the H_2O_2 Test experiment.

Conclusion

The information obtained from analysis methods performed in this study revealed that the great influence of the oxidation process towards the silver image that corroded producing redox blemishes. Gaseous peroxides emitted from poor storing material or from natural aging are the main reason of forming redox blemishes.

The obtained results showed that hydrogen peroxide causes more serious decay to the sensitizing layer comparing to the gelatin layer and the film base. The peroxide test performed caused reddening of the background next to characters revealing the formation of redox blemishes type 4, also distorted to fill the space between characters that conformed forming type 5 of redox blemishes as well on cellulose acetate film samples.

The analysis proved that the gelatin layer for film bases were not decayed by oxidation even they showed a slight degradation due to hydrolysis because if the high RH included to the hydrogen peroxide test. This proved that only the silver image is susceptible to oxidation process that leads to formation of redox blemishes.

Sputtering coating carried out for film as a sacrifice layer showed good results in preventing the oxidation after performing hydrogen peroxide test for film samples. Furthermore, using copper as a sputtering target showed better results comparing to using zinc.

Future work of sputtering coating will include different types of sputtering targets at different time intervals that might provide more preventive to oxidation process for film image.

Acknowledgment

The authors would like to express their deepest gratitude to Misr El Kheir Foundation, Egypt and Prof. Enrico Ciliberto (Chemistry Department, Catania University) for their fund and for their financial support in my studies and research. Mr. Hany Abbas and Mr. Abd-Elqader Helmy (Ahram Newspaper Microfilm Archive) Mr. Abd El-Moniem (Akhbar-Alyoum Newspaper Microfilm Archive), Dr. Francis Amin, Dr. Mourad Fawzy (Cairo University) Dr. Sherif Omar (Cairo University), Mick Newnham (National Film & Sound Archive of Australia), Dr. Maria Grazia (Catania University), Dr. Enrico Greco (Catania University), and Prof. Ezio Viscuzo (Catania University) for their greatly assistance.

References

[1] E. Kodak, *Storage and preservation of microfilms*, **Micrographic Quality D-31**, (1981), pp. 2.
[2] M. Ryhl-Svendsen, *Pollution in the photographic archive-a practical approach to the problem, IAQ in Museums and Archives*, **Proceedings of IADA Congress Preprints**, 1999, pp. 211-214.
[3] K. Hendriks, *Notes on Microfilm*, **Archivaria**, **23**, 1986, pp. 179-183.
[4] R. Hofmann, H. Wiesner**, Bestandserhaltung in archiven und bibliotheken**, Beuth Verlag, 2015, p. 310.
[5] J. Reilly, D. Nishimura, K. Cupriks, P. Adelstein, *Stability of black-and-white photographic images, with special reference to microfilm*, **Microform & Imaging Review**, **17**(5), 1988, pp. 270-278.

[6] B. Chudnovsky, **Transmission, Distribution, and Renewable Energy Generation Power Equipment,** Productivity Press, 2017, pp. 450.
[7] P. Francis, **Cathodic Protection**, National Physical Laboratory, 2007, p. 1. http://www.npl.co.uk/lmm/corrosion_control, acedido em Abril de
[8] S. Ghosh, A.K. Rakshit, **Physical Chemistry. Electrochemistry II: Voltaic or Galvanic Cells**, 2007, p. 11.
[9] Z. Laughlin, M. Conreen, H. Witchel, M. Miodownik, *The use of standard electrode potentials to predict the taste of solid metals*, **Food Quality and Preference**, **22**(7), 2011, pp 628-637.
[10] M. Friz, F. Waibel, **Coating Materials, In Optical Interference Coatings,** Springer Berlin Heidelberg, 2003, pp. 105- 108.
[11] A. Moarrefzadeh, M. Branch, *Simulation and Modeling of Physical Vapor Deposition (PVD) Process*, **WSEAS Transactions on Applied and Theoretical Mechanics**, **7**(2), 2012, pp. 106-111.
[12] E. Särhammar, *Sputtering and Characterization of Complex Multi-element Coatings*, **PhD Thesis**, Acta Universitatis Upsaliensis, 2014, pp. 16-30.
[13] P. Adelstein., J. Reilly, D. Nishimura, K. Cupriks, *Hydrogen Peroxide Test to Evaluate Redox Blemishes Formation on Processed Microfilm*, **Journal of Imaging Technology**, **17**(3), 1991, pp. 91-98.
[14] E. Gómez-Sánchez, S. Kunz, S. Simon , *ATR/FT-IR spectroscopy for the characterisation of magnetic tape materials*, **Spectroscopy Europe, 24,** 2012, pp. 6-16.
[15] M. Derrick, *Evaluation of the state of degradation of Dead Sea Scroll samples using FT-IR spectroscopy*, **The Book and Paper Group Annual**, **10**, 199, pp. 49-65.
[16] A. Adochitei, G. Drochioiu, *Rapid characterization of peptide secondary structure by FT-IR spectroscopy*, **Revue Roumanie de Chimie**, **56(**8), 2011, pp. 783-791.
[17] M.F. Valverde, **Photographic Negatives, Nature and Evolution of Processes**, Mellon Advanced Residency Program in Photograph Conservation, Image Permanence Institue, 2005, pp. 21-51.
[18] C.J. Malm, L. J. Tanghe, B.C. Laird, *Preparation of cellulose acetate-Action of sulfuric acid*, **Industrial & Engineering Chemistry**, **38**(1), 1946, pp. 77-82.
[19] * * *, **Acetate Film Deterioration, Diagnosis and Storage**, Library preservation at Harvard http://library.harvard.edu/sites/default/files/HLPS_acetatefilm.pdf, (2007), pp. 2.
[20] A. González, C. Noguez, J. Beránek, J., A. Barnard, Size, shape, stability, and color of plasmonic silver nanoparticles, **Journal of Physical Chemistry C**, **118**(17), 2014, pp. 9128-9126.

Received: May 06, 2018
Accepted: May 25, 2019